Role of Artificial Viscosity in Euler and Navier-Stokes Solvers

Aparajit J. Mahajan,* Earl H. Dowell,† and Donald B. Bliss‡
Duke University, Durham, North Carolina 27706

A method is proposed to determine directly the amount of artificial viscosity needed for stability using an eigenvalue analysis for a finite difference representation of the Navier-Stokes equations. The stability and growth of small perturbations about a steady flow over airfoils are analyzed for various amounts of artificial viscosity. The eigenvalues were determined for a small time-dependent perturbation about a steady inviscid flow over a NACA 0012 airfoil at a Mach number of 0.8 and angle of attack of 0 deg. The method has been applied to inviscid flows here, but as discussed is also applicable to viscous flows. The movement of the eigenvalue constellation with respect to the amount of artificial viscosity is studied. The stability boundaries as a function of the amount of artificial viscosity from both the eigenvalue analysis and the time-marching scheme are also presented. The eigenvalue procedure not only allows for determining the effect of varying amounts of artificial viscosity, but also for the effects of different forms of artificial viscosity.

Nomenclature

a	= speed of sound
e	= total energy per unit volume
I	= identity matrix
J	= Jacobian of transformation
M	= Mach number
p	= pressure
Re	= Reynolds number, $\rho_\infty V_\infty c/\mu_\infty$
t	= nondimensional physical time
u,v	= Cartesian velocity components
x,y	= physical Cartesian coordinates
α	= angle of attack
δ	= finite difference operator
ϵ_E, ϵ_I	= coefficients of artificial viscosity
λ	= eigenvalues
μ	= viscosity coefficient
ξ, η	= transformed coordinates
ρ	= density
τ	= transformed time

Introduction

CONSIDERABLE research has been conducted during the last few years to develop methods to solve the Navier-Stokes equations. Unsteady, separated, transonic flow over airfoils has been one of the areas receiving substantial attention. Finite difference schemes or finite element techniques are used to solve the Navier-Stokes equations.[1,2] These methods involve a numerical description of the governing equations, a finite number of grid points or elements in the flowfield, and a linear or iterative treatment of nonlinear terms.[3] These solution algorithms usually have stability problems when a computation is initiated with approximate starting data or when the finite spatial discretization is unable to resolve large gradients in flow variables. The Fourier (von Neumann) method and the matrix method of analysis are commonly used for simple equations to determine stability of a solution algorithm. In the case of the Navier-Stokes equations, the complex nonlinear nature of the governing equations and boundary conditions makes such use impossible.

The stability analysis of the solution algorithms for the Navier-Stokes equations is usually done by applying these algorithms to the wave equation or heat equation and studying their stability. Then these algorithms are implemented for the Navier-Stokes equations and artificial viscosity terms in various forms are added so as to obtain stable solutions for many different flow cases. These artificial viscosity terms are often modified to allow for shock resolution, finite spatial discretization, and experimental verification. It must be noted that artificial viscosity tends to reduce all gradients in the solution whether physically correct or numerically induced.

Pulliam[4] studied different artificial viscosity models for an Euler solver. He stabilized the Euler code with the use of artificial dissipation and studied its effect on differencing schemes and shock resolution. Dulikravich[5] analyzed the artificial dissipation models for the transonic full-potential equation and calculated the effects of these additional terms on the full-potential equation. He compared three different artificial dissipation models with physical dissipation for the compressible Navier-Stokes equations[6] and six different artificial dissipation sensors for the Euler equations.[7] These artificial dissipation models are summarized in Ref. 8. Kandil[9] studied the influence of explicit second- and fourth-order numerical dissipation terms on the Euler equations. Raj[10] investigated the sensitivity of external flow solutions to three numerical dissipation schemes using a three-dimensional Euler solver. Caughey and Turkel[11] analyzed the effect of high aspect ratio grids on the amount of artificial dissipation introduced in viscous flow computations. Most of these efforts involved time marching the codes numerous times to see the effect of artificial dissipation on solutions. Merriam[12] developed a direct quantitative method to analyze the solution stability based on the cell entropy production.

In the present work, an eigenvalue stability analysis is applied to a Navier-Stokes solver for flow over airfoils. The effect of artificial viscosity terms is studied to determine the effect on stability of time marching the solution, and also the effect on stability as indicated by the eigenvalue calculation. The study is intended to help make the utilization of artificial viscosity terms more of a science than an art.

The importance of artificial viscosity on a solution can be examined by looking at the steady-state flow values obtained in time-marching fashion. The Navier-Stokes solver, presented in the next section, was run to calculate a steady-state inviscid flow solution for a NACA 0012 airfoil at $M = 0.8$. Depending on the amount of artificial viscosity, the steady-

Received Nov. 20, 1989; revision received May 15, 1990; accepted for publication May 20, 1990.

*Research Assistant, Department of Mechanical Engineering and Materials Science; presently at the University of Toledo and NASA Lewis Research Center.

†Professor and Dean, School of Engineering. Fellow AIAA.

‡Associate Professor, Department of Mechanical Engineering and Materials Science. Member AIAA.

state values of lift and moment coefficients changed by 5%. These results are listed in Table 1. If artificial viscosity can influence the steady-state solution so much, its effect on the transient solution may be much more pronounced. Since the main purpose of artificial viscosity is to stabilize the transient solution, its effects need to be examined and understood in a systematic manner.

Analysis

A Navier-Stokes code capable of calculating unsteady, transonic and separated flows for different airfoil motions, such as pitching and plunging, was selected for the eigenvalue analysis. This finite difference, time-marching code was developed by Sankar and Tang[13] based on the Beam-Warming algorithm. This code solves the unsteady, two-dimensional Navier-Stokes equations on a body-fitted moving coordinate system in a strong conservative form using the alternate direction implicit (ADI) procedure with approximate factorization.[3] The convective terms are treated implicitly and the viscous terms are treated explicitly. This code is one of a number of Navier-Stokes solvers currently in use for transonic, viscous, unsteady problems. It has received wide attention from the aerodynamic research community. Only those parts of the Navier-Stokes solver essential for understanding the present work will be described.

All of the calculations are performed in a transformed coordinate system (ξ, η, τ) that is linked to the moving, body-fitted coordinate system as follows:

$$\xi = \xi\,(x,y,t), \qquad \eta = \eta\,(x,y,t) \qquad \tau = \tau(t) \tag{1}$$

The two-dimensional, unsteady Navier-Stokes equations in the transformed coordinate system are written as

$$\tilde{q}_\tau + \tilde{F}_\xi + \tilde{G}_\eta = \tilde{R}_\xi + \tilde{S}_\eta \tag{2}$$

where

$$\tilde{q} = J^{-1}\,\{\rho,\ \rho u,\ \rho v,\ e\}^T \tag{3}$$

The quantities $\tilde{F}$, $\tilde{G}$ are the convection terms and $\tilde{R}$, $\tilde{S}$ the viscous terms. In Eq. (2), central differencing is used for spatial derivatives and forward differencing is used for time derivatives. The resulting equation in the discretized form at any point (i,j) is

$$\frac{\Delta\tilde{q}_{ij}^{n+1}}{\Delta\tau} + \delta_\xi \tilde{F}_{ij}^{n+1} + \delta_\eta \tilde{G}_{ij}^{n+1} = \delta_\xi \tilde{R}_{ij}^{n+1} + \delta_\eta \tilde{S}_{ij}^{n+1} - \epsilon_E D_{ij}^n \tag{4}$$

Table 1 Effect of artificial viscosity on steady-state lift, moment, and drag coefficients (NACA 0012 airfoil, $M = 0.8$, inviscid flow)

α deg	ϵ_E	ϵ_I	C_l	C_m	C_d
	2	10	0.5189957	-0.0746779	0.0466132
	3	15	0.5127812	-0.0729532	0.0458576
2	4	20	0.5082933	-0.0715801	0.0452502
	5	25	0.5038787	-0.0704199	0.0448124
	6	30	0.5003532	-0.0695243	0.0444229
	2	10	0.9343331	-0.1737796	0.1108001
	3	15	0.9259864	-0.1703883	0.1092868
4	4	20	0.9203443	-0.1682357	0.1082361
	5	25	0.9143991	-0.1659712	0.1072367
	6	30	0.9091913	-0.1640378	0.1063879
	2	10	1.21352879	-0.2419128	0.18253395
	3	15	1.20526286	-0.2380901	0.18060031
6	4	20	1.19826546	-0.2348858	0.17901815
	6	30	1.18628397	-0.2295509	0.17644304
	2	10		code was unstable	
	3	15	1.3956165	-0.2741378	0.2529984
8	4	20	1.3891096	-0.2710383	0.2511782
	6	30	1.3760950	-0.2648963	0.2748513

where $\Delta\tilde{q}_{ij}^{n+1} = \tilde{q}_{ij}^{n+1} - \tilde{q}_{ij}^n$, and the superscripts n and $n+1$ refer to two successive time levels. The artificial viscosity term D, contains spatial derivatives of second- and fourth-order and ϵ_E controls the amount of this *explicit* artificial viscosity. The highly nonlinear terms F and G are then expanded in a Taylor series about time level n. The resulting equation is then approximately factored into two operators so as to allow for two sweeps, a $\xi-$ and an $\eta-$sweep, during which block tridiagonal matrix equations are solved. To allow for the explicit treatment of the viscous terms, implicit smoothing terms are added to the left-hand side of Eq. (4). These terms contain spatial derivatives of second-order and ϵ_I controls the amount of *implicit* smoothing. The final form of the governing equation is

$$\{I + \Delta\tau[\delta_\xi A - (\epsilon_I/J)\,\delta_{\xi\xi}J]\}\,\{I + \Delta\tau[\delta_\eta B - (\epsilon_I/J)\delta_{\eta\eta}J]\}\Delta\tilde{q}^{n+1}$$
$$= \left[-(\delta_\xi \tilde{F}^n + \delta_\eta \tilde{G}^n) + \delta_\xi \tilde{R}^n + \delta_\eta \tilde{S}^n - \epsilon_E D^n\right]\Delta\tau \tag{5}$$

where

$$A = \left[\frac{\partial\tilde{F}}{\partial\tilde{q}}\right]^n, \qquad B = \left[\frac{\partial\tilde{G}}{\partial\tilde{q}}\right]^n$$

This formulation can model time-accurate viscous flows for sufficiently small time steps. The implicit treatment of viscous terms would allow larger time steps for time-accurate viscous flow computations.

All of the boundary conditions are explicitly applied at each time step. At the far-field boundaries, except in the downstream boundary, the flowfield is assumed to be undisturbed. At the downstream boundary, the velocity field u, v, and the entropy are extrapolated from the interior, so as to allow for vorticity transport. The pressure at the downstream boundary is prescribed to be freestream pressure. On the solid boundary, for inviscid flows, the normal velocity is set to zero and, for viscous flows, the normal and tangential velocities are set to zero. The density is extrapolated from the interior. For calculation of viscous, turbulent flows, a two-layer Baldwin-Lomax eddy viscosity model[14] is used.

Artificial Viscosity Terms

In this Navier-Stokes solver, an adaptive dissipation scheme as proposed by Jameson et al.[15] is used. The dissipation terms are written, in conservation form, as a combination of second- and fourth-order terms. A sensor, based on the second derivative of pressure, turns on the second-order dissipation term in the vicinity of shocks and suppresses the fourth-order dissipation term. Jameson's approach leads to crisp, three-point shocks in most cases without overshoots. This switching was employed only in the streamwise (ξ-) direction in this Navier-Stokes solver. The dissipation term is written as

$$D_{ij} = J^{-1}\,\delta_{\eta\eta\eta\eta}(J\tilde{q}) + \delta_\xi\frac{C_1}{J_{i+1/2,j}}(q_{i+2,j} - 3q_{i+1,j}$$
$$+ 3q_{ij} - q_{i-1,j}) - \frac{C_2}{J_{i+1/2,j}}(q_{i+1,j} - q_{ij}) \tag{6}$$

where

$$C_2 = \max\,(\beta_{ij},\ \beta_{i+1,j})$$

and

$$\beta_{ij} = H\frac{|(p_{i+1,j} - 2p_{ij} + p_{i-1,j})|}{(p_{i+1,j} - 2p_{ij} + p_{i-1,j})}$$

and

$$C_1 = \max\,(0,\ 1 - C_2)$$

Here H is a user-input value, of the order of 10. The quantity β_{ij} senses the second derivative of pressure and is large only near shocks. This leads to a nonzero value of C_1, near shocks.

The value $J_{i+1/2,j}$ needed in the preceding calculation is computed as

$$\frac{1}{J_{i+1/2,j}} = \frac{1}{2}\left(\frac{1}{J_{ij}} + \frac{1}{J_{i+1,j}}\right) \tag{7}$$

Eigenvalue Problem

To analyze the stability of the solution procedure, an eigenvalue problem is formulated for the Navier-Stokes code. The details for the formulation and calculation procedure are given is a separate paper.[16] For the sake of brevity, clarity, and also in the limit of Δt going to 0, it is described for Eq. (3) instead of Eq. (5). Since $\tilde{F}$, $\tilde{G}$, $\tilde{R}$, and $\tilde{S}$ are functions of $\tilde{q}$, Eq. (3) can be rewritten as

$$\tilde{q}_\tau = -\tilde{F}_\xi - \tilde{G}_\eta + \tilde{R}_\xi + \tilde{S}_\eta = \tilde{Q}\,(\tilde{q}) \tag{8}$$

Here $\tilde{Q}\,(\tilde{q})$ also contains the artificial viscosity terms. For small perturbations about steady flow, the following eigenvalue problem results. Substitute $\tilde{q} = \bar{q} + \hat{q}$ in Eq. (8), where $\bar{q}$ is steady-state value and $\hat{q}$ a small perturbation. This gives

$$\hat{q}_\tau = \tilde{Q}\,(\bar{q}) + \left[\frac{d\tilde{Q}}{d\tilde{q}}\right]_{\bar{q}} \hat{q} \tag{9}$$

At steady-state flow conditions, $\tilde{Q}\,(\bar{q}) = 0$ which reduces Eq. (9) to

$$\hat{q}_\tau = \left[\frac{d\tilde{Q}}{d\tilde{q}}\right]_{\bar{q}} \hat{q} \tag{10}$$

Substituting $\hat{q} = q\,e^{\lambda t}$ in Eq. (10) gives

$$\lambda q e^{\lambda\tau} = \left[\frac{d\tilde{Q}}{d\tilde{q}}\right]_{\bar{q}} q\,e^{\lambda\tau} \tag{11}$$

Equation (11) can be written in matrix form as

$$\lambda\,\{q\} = [P]\,\{q\} \tag{12}$$

The matrix $[P]$ contains the spatial derivatives of the flux Jacobians and artificial viscosity terms. The flux Jacobians can be expressed analytically and then evaluated numerically or they can be calculated in a direct numerical fashion with no analytical expressions for derivatives. In the present work, the derivatives have analytical expressions and are evaluated from the steady-state flowfield. The use of Baldwin-Lomax turbulence model in viscous terms does not allow analytical evaluation of viscous flux Jacobians, as viscosity is an empirical function of $\{q\}$. The numerical determination of viscous flux Jacobians is computationally very expensive, and hence, the procedure is demonstrated for inviscid flows here.

This eigenvalue problem corresponds to flow over airfoils, for example, and when solved provides the information required for the stability analysis of the time-marching procedure.

Results and Discussion

In Eq. (12), $[P]$ is a sparse, real, nonsymmetric matrix of order n, where $n = 4 \times imax \times jmax \approx 24{,}000$. The state-of-the-art software available for eigenvalue calculation (EISPACK, etc.) is *not* capable of storing a 24,000 × 24,000 matrix or utilizing the sparsity and nonsymmetry of the present problem for obtaining a solution with reasonable computer time. A procedure that would exploit the sparsity of the matrix for storage and calculation purposes is needed. The iterative methods, for eigenvalue calculations on this scale, need a very good initial guess for convergence. Also they are not capable of providing spectral information about the eigenvalues. The "reduction-to-condensed forms" methods, however, provide a suitable procedure to attempt a solution to this eigenvalue problem.

A modified Lanczos recursive procedure with no reorthogonalization is used to calculate the eigenvalues. For very large real, symmetric matrices, the Lanczos procedure is one of the most widely used ways to estimate the eigenvalues due to its efficiency and range of eigenvalues calculated.[17] This procedure was modified by Cullum and Willoughby[18] for nonsymmetric matrices. A family of complex, symmetric, tridiagonal matrices that represent orthogonal projections of the given original matrix $[P]$ onto the corresponding Krylov subspaces are calculated during this recursive procedure. The eigenvalues of these Lanczos matrices are the eigenvalues of the operators obtained for $[P]$ by restricting $[P]$ to the Krylov subspaces. These eigenvalues are found to be independent of the starting vectors used in the recursion. This procedure was compared with a lopsided iteration eigenvalue calculation procedure. The accuracy and validity of this eigenvalue calculation procedure are discussed in detail in a separate paper.[16]

The eigenvalues correspond to a transient solution and are affected by the choice of ϵ_E and ϵ_I in the transient solution. The converged steady-state solution is obtained using $\epsilon_E = 2$ and $\epsilon_I = 10$. This steady-state solution is sufficiently independent of ϵ_E and ϵ_I, so that the eigenvalues of the transient solution are not affected by the choice of ϵ_E and ϵ_I in the steady-state solution. The eigenvalues obtained for a NACA 0012 airfoil at $M = 0.8$, $\alpha = 0$ deg, and artificial viscosity parameters $\epsilon_E = 0$ and $\epsilon_I = 0$ for inviscid flow are shown in Fig. 1. Some of these eigenvalues have a positive real part,

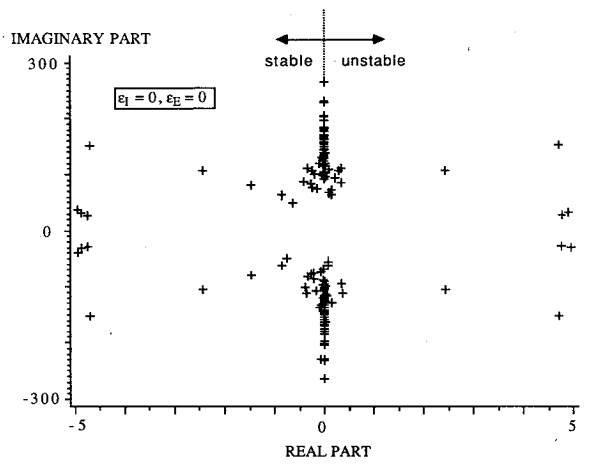

Fig. 1 Eigenvalue constellation for $\epsilon_I = 0$ and $\epsilon_E = 0$ (NACA 0012 airfoil, $M = 0.8$, inviscid flow, $\alpha = 0$ deg).

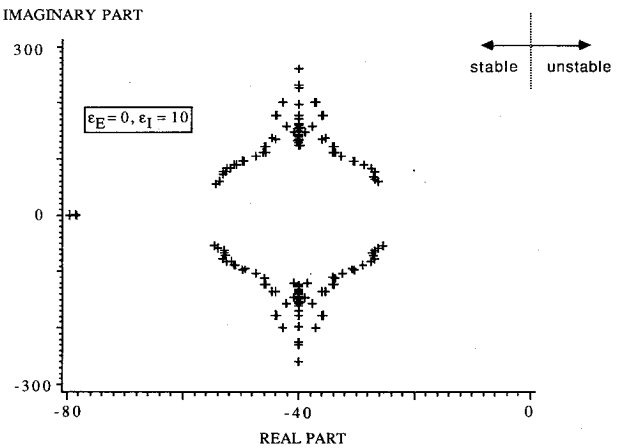

Fig. 2 Eigenvalue constellation for $\epsilon_I = 10$ and $\epsilon_E = 0$ (NACA 0012 airfoil, $M = 0.8$, inviscid flow, $\alpha = 0$ deg).

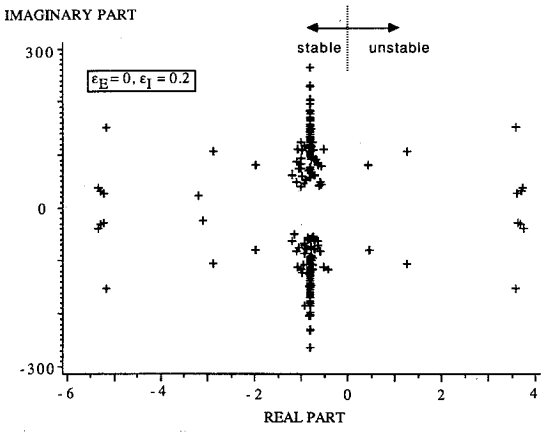

Fig. 3 Eigenvalue constellation for $\epsilon_I = 0.2$ and $\epsilon_E = 0$ (NACA 0012 airfoil, $M = 0.8$, inviscid flow, $\alpha = 0$ deg).

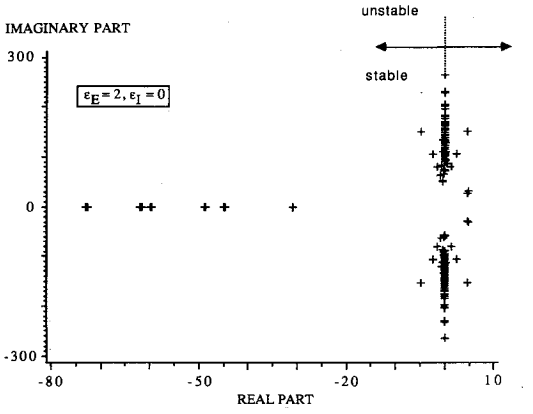

Fig. 4 Eigenvalue constellation for $\epsilon_I = 0$ and $\epsilon_E = 2$ (NACA 0012 airfoil, $M = 0.8$, inviscid flow, $\alpha = 0$ deg).

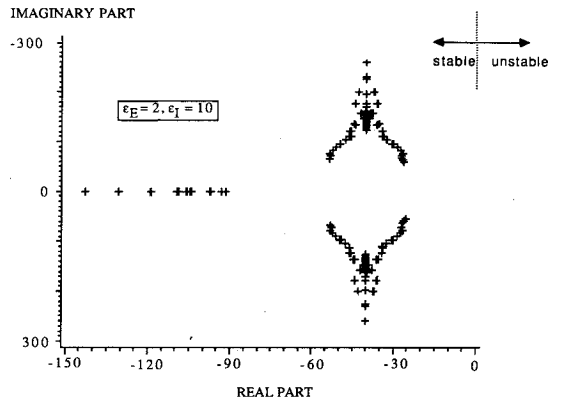

Fig. 5 Eigenvalue constellation for $\epsilon_I = 10$ and $\epsilon_E = 2$ (NACA 0012 airfoil, $M = 0.8$, inviscid flow, $\alpha = 0$ deg).

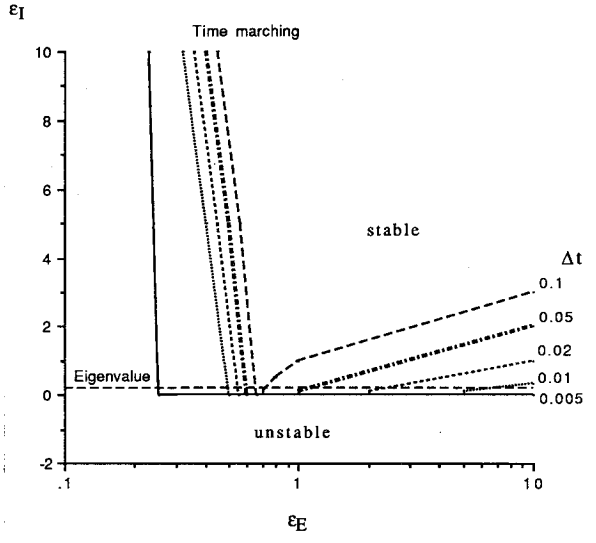

Fig. 6 Stability boundary as a function of (ϵ_E, ϵ_I) for different time stepsizes.

which corresponds to an instability in the Navier-Stokes code. This instability is further studied by systematically varying the artificial viscosity in the Navier-Stokes code. The two parameters that represent the artificial viscosity in the time-marching code are 1) implicit smoothing terms ϵ_I consisting of second-order spatial derivatives and 2) explicit artificial viscosity ϵ_E mostly consisting of fourth-order spatial derivatives. The first parameter when set to $\epsilon_I = 10$ moved the entire eigenvalue constellation to the left, i.e., it changed the real part of all of the eigenvalues to a large negative number, thus making them stable, see Fig. 2. The movement of the eigenvalue constellation for a very small value of ϵ_I is shown in Fig. 3; it has a few unstable eigenvalues. By contrast, the second parameter when set to $\epsilon_E = 2$ stretched the eigenvalue constellation, with eigenvalues having a small imaginary part being affected most. Its effect on the eigenvalues with large imaginary parts is negligible; see Fig. 4. When both of these parameters have nonzero values, the eigenvalue constellation exhibits a combination of these two movements, as seen in Fig. 5 when $\epsilon_E = 2$ and $\epsilon_I = 10$.

It is observed that the artificial viscosity parameters that give unstable eigenvalues also make the time-marching Navier-Stokes code unstable; $\epsilon_E = 0$ and $\epsilon_I = 0$. The artificial viscosity parameters that show all stable eigenvalues also make the time-marching code stable; $\epsilon_E = 2$ and $\epsilon_I = 10$. The relationship between artificial viscosity parameters and the stability of time-marching code was further analyzed using this eigenvalue calculation. A large number of calculations with many different combinations of ϵ_E and ϵ_I were performed to obtain the stability boundaries as a function of ϵ_E and ϵ_I. In the time-marching code, these boundaries also depend on the time stepsize Δt used. The eigenvalue calculation, due to analytical treatment of time derivatives, corresponds to a time stepsize of zero. The stability boundaries in ϵ_E-ϵ_I plane are shown in Fig. 6 for $\Delta t = 0.005$, 0.01, 0.02, 0.05, and 0.1. The stability boundary from the eigenvalue calculation is also shown. It should be noted that the horizontal part of the stability boundary from the eigenvalue calculation corresponds to $\epsilon_I = 0.3 \sim 0.35$ and differs from the bottom part of the stability boundary from the time-marching calculation, which corresponds to $\epsilon_I = 0.0$. It is believed that the explanation of this difference in results between the time-marching code and the eigenvalue calculation is as follows.

Switched dissipation provides second-order damping. The amount of this second-order damping is large in the vicinity of shocks or for the transonic flows (overall flowfield). In the time-marching calculation, although $\epsilon_I = 0$, the nonzero value of ϵ_E provides the required damping for stability. It is conjectured that at lower Mach numbers (strictly subsonic flows), the eigenvalue calculation requires $\epsilon_I > 0$, as there is no appreciable second-order switched dissipation in the absence of shocks (a very small amount of second-order switched dissipation is present around the leading edge of the airfoil). A systematic study of the stability boundaries for a Mach number of 0.3, similar to the one presented here for a Mach number of 0.8, would be desirable to confirm this conjecture.

Many interesting observations can be made from Fig. 6. The stable region gets smaller as the time stepsize increases. For the time-marching code, the stability boundary is composed of three parts; namely, left, right, and bottom. For a fixed value of ϵ_I, say 1, if ϵ_E is increased from 0, first the calculation is unstable, then after crossing the boundary, it is stable and then once again it turns unstable for large enough ϵ_E. The

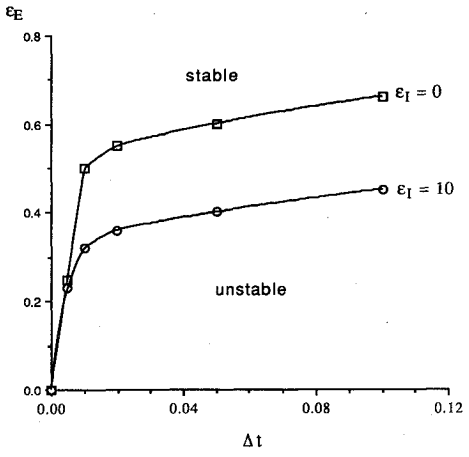

Fig. 7 Stability boundary sections in (Δt, ϵ_E) plane for different ϵ_I.

instability on the left occurs gradually after the solution has progressed for some time. The instability on the right occurs abruptly at the start of the time marching. As the time stepsize becomes smaller, the left boundary moves towards $\epsilon_E = 0$ and tends to be vertical. The right boundary moves farther to the right very rapidly and tends to be horizontal as the time stepsize decreases. The bottom boundary increases on both the sides as the time stepsize becomes smaller. To analyze this quantitatively, a section of the stability boundaries is shown in $\Delta t - \epsilon_E$ plane for two different values of ϵ_I in Fig. 7. These sections can be extrapolated to $\Delta t = 0$ for a comparison with the eigenvalue stability analysis. It can be seen that, as Δt tends to zero, the amount of artificial dissipation needed for a stable solution also tends to zero. From Figs. 6 and 7, it can be confirmed that in the limit as Δt goes to zero, the stability boundaries from both the eigenvalue and time-marching calculations are in agreement. Smaller time stepsizes than those used here could not be considered in this study, as the time-marching calculation is computationally very expensive. Furthermore, it takes a large number of time steps during time marching to determine the stability boundary as the time stepsize decreases.

Concluding Remarks

An eigenvalue problem formulation and a calculation procedure for eigenvalues are developed and applied to an Euler/Navier-Stokes solver. This procedure is capable of studying the effect of artificial viscosity on the stability of the time-marching solution technique. It can also help distinguish between the instabilities in the physical problem and those introduced by the numerical modeling and discretization. At present, the calculations are done for small time-dependent perturbations about steady flow over airfoils and the growth of these perturbations is studied. The movement of eigenvalue constellation with respect to artificial viscosity is analyzed. This movement of eigenvalues due to change in the artificial viscosity parameters is being studied further and efforts are being made to correlate it quantitatively with the rate of growth of instabilities in the time-marching code. This approach provides a direct way to analyze the stability of Navier-Stokes solvers, rather than a trial-and-error approach as is presently used by most investigators.

In the numerical results discussed here, only inviscid flows are considered. The same procedure applies to viscous flows also. At present, the viscosity model (Baldwin-Lomax turbulence model) used in the Navier-Stokes solver is of an empirical nature, making viscosity an empirical function of flow variables. Thus, to determine the contribution of viscous terms to

$$\left[\frac{d\bar{Q}}{d\bar{q}}\right]_{\bar{q}}$$

the $24{,}000 \times 24{,}000$ derivatives will have to be evaluated numerically and the computational costs are prohibitive. If an *analytical* viscosity model were used, these derivatives could be evaluated analytically to form matrix $[P]$, and the stability boundaries for viscous flows could be determined by a similar procedure at comparable computational cost. The interaction between "natural" and "artificial" viscosity can also be studied then.

Acknowledgments

This research is sponsored, in part, by the Structural Dynamics Branch at NASA Lewis Research Center under Grant NAG 3-724. Krishna Rao V. Kaza and George L. Stefko are the technical monitors. The computer time is provided, in part, by the Cornell National Supercomputing Facility.

References

[1]Anderson, D. A., Tannehill, J. C., and Pletcher, R. H., *Computational Fluid Mechanics and Heat Transfer,* Hemisphere, Washington, DC, 1984.

[2]Baker, A. J., *Finite-Element Computational Fluid Mechanics,* Hemisphere, Washington DC, 1983.

[3]Beam, R. M., and Warming, R. F., "An Implicit-Factored Scheme for the Compressible Navier-Stokes Equations," *AIAA Journal,* Vol. 16, No. 7, 1978, pp. 393-401.

[4]Pulliam, T. H., "Artificial Dissipation Models for the Euler Equations," *AIAA Journal,* Vol. 24, No. 12, 1986, pp. 1931-1940.

[5]Dulikravich, G. S., "Analysis of Artificial Dissipation Models for the Transonic Full-Potential Equation," *AIAA Journal,* Vol. 26, No. 10, 1988, pp. 1238-1245.

[6]Dulikravich, G. S., Dorney, D. J., and Lee, S., "Numerical Versus Physical Dissipation in the Solution of Compressible Navier-Stokes Equations," AIAA Paper 89-0550, Jan. 1989.

[7]Dulikravich, G. S., and Dorney, D. J., "Artificial Dissipation Sensors for Computational Gas Dynamics," AIAA Paper 89-0643, Jan. 1989.

[8]Dulikravich, G. S., "Physically Based Artificial Dissipation Concepts in Computational Fluid Dynamics," *Proceedings of the 7th International Conference on Finite-Element Methods in Flow Problems,* Univ. of Alabama, Huntsville, AL, April 1989, pp. 1199-1204.

[9]Kandil, O. A., and Chuang, A. H., "Influence of Numerical Dissipation on Computational Euler Equations for Vortex Dominated Flows," *AIAA Journal,* Vol. 25, No. 11, 1987, pp. 1426-1434.

[10]Raj, P., "An Euler Code for Nonlinear Aerodynamic Analysis—Assessment of Capabilities," Society of Automotive Engineers Paper 88-1486, Oct. 1988.

[11]Caughey, D. A., and Turkel, E., "Effects of Numerical Dissipation on Finite-Volume Solutions of Compressible Flow Problems," AIAA Paper 88-0621, Jan. 1988.

[12]Merriam, M. L., "Towards a Rigorous Approach to Artificial Dissipation," AIAA Paper 89-0471, Jan. 1989.

[13]Sankar, N. L., and Tang, W., "Numerical Solution of Unsteady Viscous Flow Past Rotor Sections," AIAA Paper 85-0129, Jan. 1985.

[14]Baldwin, B. S., and Lomax, H., "Thin-Layer Approximation and Algebraic Model for Separated Turbulent Flows," AIAA Paper 78-257, Jan. 1978.

[15]Jameson, A., Schmidt, W., and Turkel, E., "Numerical Solutions of the Euler Equations by Finite-Volume Methods Using Runge-Kutta Time-Stepping Schemes," AIAA Paper 81-1259, June 1981.

[16]Mahajan, A. J., Dowell, E. H., and Bliss, D. B., "Eigensystem Analysis Procedure for a Navier-Stokes Solver with Application to Flows over Airfoils," *Journal of Computational Physics* (submitted for publication).

[17]Wilkinson, J. H., *The Algebraic Eigenvalue Problem,* Clarendon, Oxford, England, UK 1965.

[18]Cullum, J. K., and Willoughby, R. A., "A Practical Procedure for Computing Eigenvalues of Large Sparse Nonsymmetric Matrices," *Large Scale Eigenvalue Problems*, edited by J. Cullum and R. A. Willoughby, Elsevier, New York, 1986, pp. 193-240.